Magnetic properties of amorphous $(Fe_{1-x}Co_x)_{77.5}Nd_4B_{18.5}$ alloys before and after crystallization

1992 J. Phys.: Condens. Matter 4 7247

(http://iopscience.iop.org/0953-8984/4/35/009)

J. Phys.: Condens. Matter 4 (1992) 7247–7256. Printed in the UK

Magnetic properties of amorphous $(Fe_{1-x}Co_x)_{77.5}Nd_4B_{18.5}$ alloys before and after crystallization

Shen Bao-gen, Yang Lin-yuan, Liang Jian-zhen and Guo Hui-qun

State Key Laboratory of Magnetism, Institute of Physics, Chinese Academy of Sciences, PO Box 603, Beijing 100 080, People's Republic of China

Received 17 February 1992, in final form 29 April 1992

Abstract. The magnetic properties of amorphous $(Fe_{1-x}Co_x)_{77.5}Nd_4B_{18.5}$ alloys before and after crystallization were studied. The Fe atom moment $\bar{\mu}_{Fe}$ is found to increase with increasing x from $2.0\mu_B$ for $x = 0$ to a saturation value of $2.3\mu_B$ for $x = 0.7$ and then to decrease, when the Co atom moment $\bar{\mu}_{Co}$ is assumed to be constant for all x. The variation in Fe moment is in good agreement with the Co concentration dependence of the average hyperfine field. The Curie temperature T_C is found first to increase and then to decrease, attaining a maximum value of 895 K at about $x = 0.7$. This variation in T_C with x is calculated using a phenomenological model described by Kouvel; the exchange interaction temperatures T_{Fe-Fe}, T_{Fe-Co} and T_{Co-Co} are calculated to be 584 K, 1010 K and 825 K, respectively. With increasing Co concentration x, the crystallization temperature is approximately constant for $x \leqslant 0.7$ and then increases slightly with increasing x. The crystalline phases in crystallized samples were identified by x-ray diffraction. A high room-temperature coercive field H_c and a high energy product $(BH)_{max}$ for the optimally annealed samples are obtained.

1. Introduction

In recent years, a number of investigations [1–6] have been reported on the magnetic properties and crystallization behaviours of amorphous Fe–Nd–B alloys with a low Nd concentration. Coehoorn and co-workers [1, 2] have studied the structures and magnetic properties of crystallized amorphous melt-spun ribbons of the approximate composition $Nd_4Fe_{78}B_{18}$ and have found an energy product of 11.7 MGOe in amorphous $Nd_4Fe_{80}B_{20}$ alloy after crystallization by annealing at 670 °C for 30 min. Shen and co-workers [3–6] have studied the magnetic properties and crystallization behaviours of amorphous Fe–Nd–B alloys over a wide composition range and obtained a room-temperature coercive field of 3 kOe and a maximum energy product of 13.3 MGOe in the optimally annealed Fe–Nd–B alloys with a low Nd concentration of 4.5 at.%. A non-collinear spin arrangement, which was first proposed by Coey *et al* [7], has been accepted to explain the magnetic properties of amorphous $(Fe_{1-x}Nd_x)_{81.5}B_{18.5}$ alloys [8]. The Curie temperature of amorphous $Nd_4Fe_{96-x}B_x$ alloys shows a maximum value of 622 K at about $x = 25$ [5], whereas the Curie temperature of amorphous $(Fe_{1-x}Nd_x)_{81.5}B_{18.5}$ alloys appears to decrease monotonically with increasing Nd concentration [8]. The results of a study on the effects of substitutions of Fe by B, Al, Ga, Co and Ni on the magnetic properties of amorphous and crystallized $Fe_{77.5}Nd_4B_{18.5}$ alloy have been reported in an attempt to increase

0953-8984/92/357247+10$04.50

the magnetic hardness and stability of these alloys, but this was not possible as most of these substitutions result in decreases in the coercive field and energy product. Some results of investigations on rapidly quenched $(Fe_{1-x}Co_x)_{77.5}Nd_4B_{18.5}$ alloys with $x \leqslant 0.4$ have been reported [9]. The crystallized Fe–Co–Nd–B alloys with a low Co concentration show a high coercive field and a high energy product at room temperature. The Co substitution for Fe results in an increase in T_C of the hard magnetic phase, improving the thermostability of these materials. In this paper, we report the magnetic propeties and Mössbauer spectra of amorphous $(Fe_{1-x}Co_x)_{77.5}Nd_4B_{18.5}$ alloys and their crystallization behaviours over the whole composition range from $x = 0$ to $x = 1.0$.

2. Experimental details

Iron (purity, 99.9%), cobalt (purity, 99.9%), neodymium (purity, 99.9%) and Fe–B alloy (purity, 98.6%) were melted by arc melting in an argon atmosphere of high purity into homogeneous buttons with the compositions $(Fe_{1-x}Co_x)_{77.5}Nd_4B_{18.5}$ ($0 < x < 1.0$). Amorphous ribbons about 1 mm wide and 20 μm thick were prepared by melt spinning in an argon atmosphere in a polished Cu drum of 20 cm diameter with a speed of about 47 m s^{-1} and were then annealed in a steel tube in a vacuum of 10^{-5} Torr at different temperatures and times.

High-field magnetization measurements at 1.5 K were made on these amorphous samples using an extracting-sample magnetometer in fields ranging from 0 to 65 kOe. The ^{57}Fe Mössbauer spectra at 77 K for the amorphous alloys were obtained using a constant-acceleration spectrometer with a 50 mCi source of ^{57}Co in palladium. The velocity scale was calibrated using an α-Fe absorber at room temperature. The Curie temperatures of the amorphous alloys were determined from the temperature dependence of the magnetization and AC susceptibility. The crystallization temperatures were measured by differential scanning calorimetry (DSC) at a heating rate of 20 K min^{-1}. The room-temperature hysteresis loops of the annealed samples were measured in a vibrating-sample magnetometer. The crystalline phases of the heat-treated samples were identified by x-ray diffraction with Co Kα radiation.

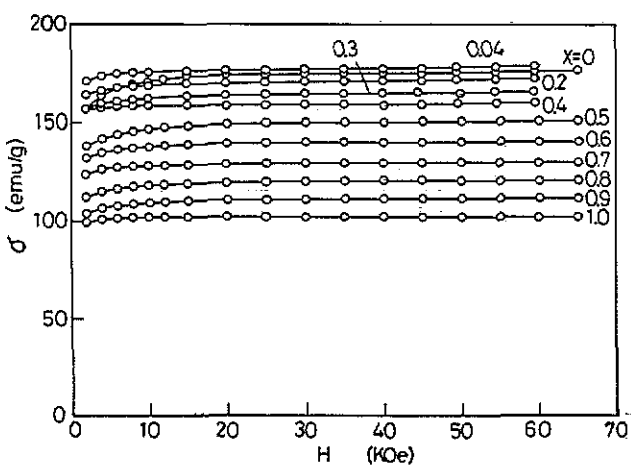

Figure 1. Magnetization curves of amorphous $(Fe_{1-x}Co_x)_{77.5}Nd_4B_{18.5}$ alloys at 1.5 K.

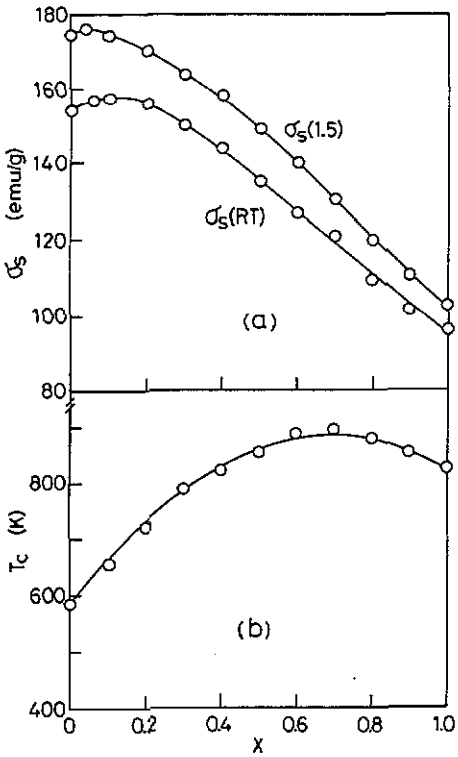

Figure 2. (*a*) Saturation magnetizations $\sigma_s(1.5)$ at 1.5 K and σ_s(RT) at room temperature, and (*b*) the Curie temperature T_C for amorphous $(Fe_{1-x}Co_x)_{77.5}Nd_4B_{18.5}$ alloys as functions of the Co concentration x.

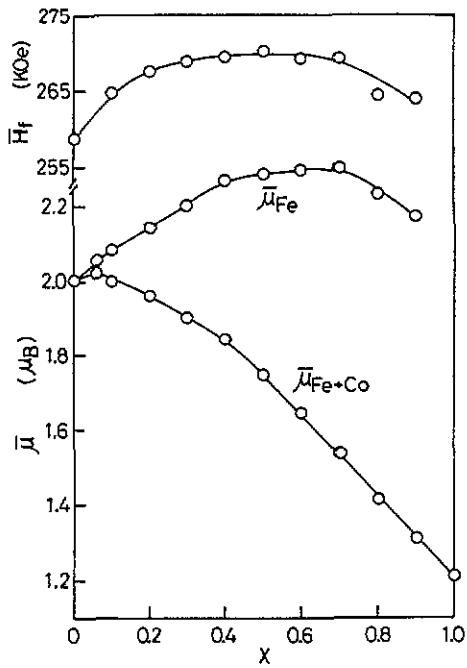

Figure 3. Magnetic moments $\bar{\mu}_{Fe+Co}$ and $\bar{\mu}_{Fe}$ and the average hyperfine field $\bar{H}_f$ at 77 K for amorphous $(Fe_{1-x}Co_x)_{77.5}Nd_4B_{18.5}$ alloys as functions of the Co concentration x, where the Co atom moment is assumed to be constant ($\bar{\mu}_{Co} = 1.21\mu_B$).

3. Results and discussion

3.1. Magnetic moment

Figure 1 shows the magnetization σ at 1.5 K as a function of the external field H for amorphous $(Fe_{1-x}Co_x)_{77.5}Nd_4B_{18.5}$ alloys. The saturation magnetizations $\sigma_s(1.5)$ were obtained by fitting the experimental data of $\sigma(H)$ against H using the law of approach to saturation:

$$\sigma(H) = \sigma_s(1 - a/H - b/H^2) \tag{1}$$

where $\sigma(H)$ is the magnetization at the magnetic field H. The saturation magnetization $\sigma_s(1.5)$ at 1.5 K is shown in figure 2(*a*) as a function of Co concentration x, together with the saturation magnetization σ_s(RT) measured at room temperature in a magnetic field of 12 kOe. The σ_s-values have maxima which, at low Co concentrations, are similar to the results for crystalline Fe–Co compounds and other amorphous Fe–Co-based alloys [10].

The average magnetic moments per magnetic atom of $(Fe_{1-x}Co_x)_{77.5}Nd_4B_{18.5}$ amorphous alloys were calculated using the values of $\sigma_s(1.5)$. According to previous work, it has been shown that, in the amorphous alloys containing a rare-earth metal,

the moments of RE atoms exhibit a non-collinear structure [7, 8, 11]. The magnetic moment per Nd atom in amorphous $(Fe_{1-x}Co_x)_{77.5}Nd_4B_{18.5}$ alloys is suggested to be $1.05\mu_B$ [9]. Thus, the average magnetic moment $\bar{\mu}_{Fe+Co}$ per Fe+Co atom is obtained, as shown in figure 3. The composition dependence of the average moment $\bar{\mu}_{Fe+Co}$ may be written as

$$\bar{\mu}_{Fe+Co} = \bar{\mu}_{Fe}(1-x) + \bar{\mu}_{Co}x \tag{2}$$

where $\bar{\mu}_{Fe}$ and $\bar{\mu}_{Co}$ are the effective magnetic moments per Fe atom and per Co atom, respectively. Collins and Forsyth [12] studied the magnetic properties of the crystalline Fe–Co alloys using polarized neutron diffraction and found that the average moment $\bar{\mu}_{Fe}$ per Fe atom rises from $2.2\mu_B$ for pure Fe to just over $3\mu_B$ for alloys with 50 at.% Co or higher, and the average moment $\bar{\mu}_{Co}$ per Co atom remains at an essentially constant value of $1.8\mu_B$. The rise in $\bar{\mu}_{Fe}$ with increasing Co concentration has been reported by Guo *et al* [13] for amorphous $(Fe_{1-x}Co_x)_{78}Si_{9.5}B_{12.5}$ alloys in which the Co atom moment is $1.21\mu_B$. For amorphous $Co_{77.5}Nd_4B_{18.5}$ alloy with $x = 1.0$, $\bar{\mu}_{Co}$ is found to be $1.21\mu_B$. If $\bar{\mu}_{Co}$ of amorphous $(Fe_{1-x}Co_x)_{77.5}Nd_4B_{18.5}$ alloys is assumed to keep the value of $1.21\mu_B$ over the whole concentration, the composition dependence of $\bar{\mu}_{Fe}$ can be obtained from equation (2), as can be seen in figure 3. $\bar{\mu}_{Fe}$ is found to increase with increasing Co concentration from $2.0\mu_B$ for $x = 0$ to a saturation value of $2.3\mu_B$ for $x = 0.7$ and then to decrease.

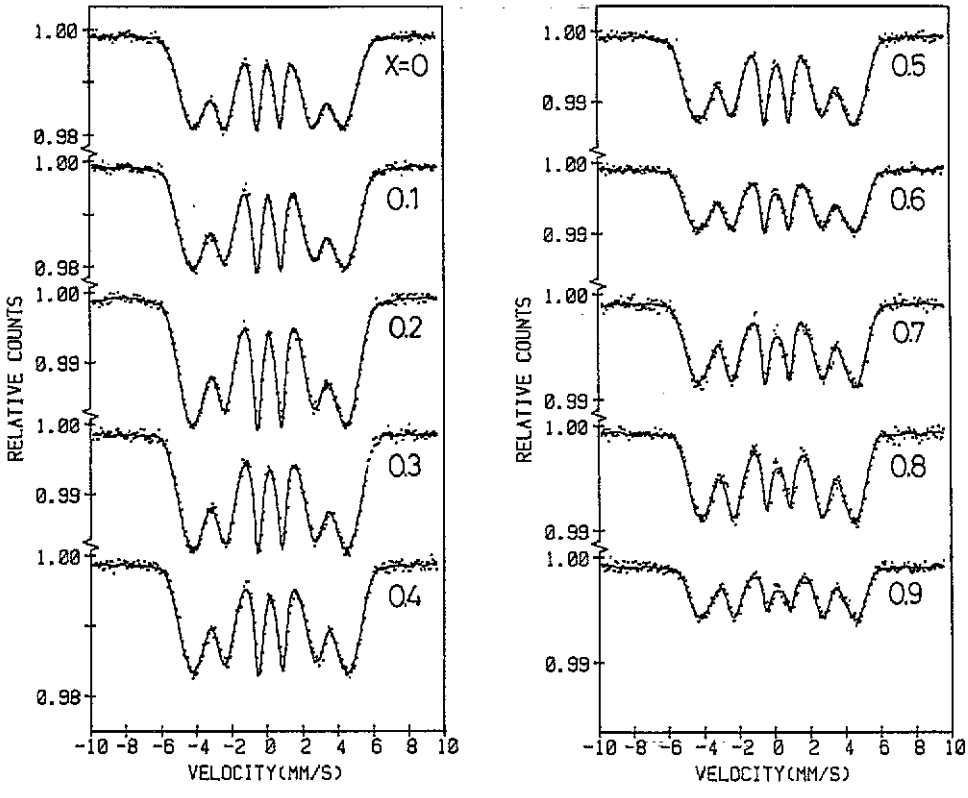

Figure 4. Mössbauer spectra of amorphous $(Fe_{1-x}Co_x)_{77.5}Nd_4B_{18.5}$ alloys measured at 77 K.

Figure 4 shows Mössbauer spectra of amorphous $(Fe_{1-x}Co_x)_{77.5}Nd_4B_{18.5}$ alloys measured at 77 K. These spectra are typical of the spectra obtained for ferromagnetic amorphous alloys. They show broadened lines due to the occurrence of hyperfine field distributions. The hyperfine field distribution $P(H)$, which is fitted by using the least-squares method, is shown in figure 5 for all samples with $x \leqslant 0.9$. From the resultant $P(H)$, one can calculate the average hyperfine field $\bar{H}_f$, defined as

$$\bar{H}_f = \int P(H) H \, dH. \tag{3}$$

$\bar{H}_f$ is found to increase at first and then to decrease with increasing Co concentration, as shown in figure 3. This variation in $\bar{H}_f$ with x is in good agreement with the Co concentration dependence of $\bar{\mu}_{Fe}$. Similar results have also been observed for amorphous $(Fe_{1-x}Co_x)_{78}Si_{9.5}B_{12.5}$ alloys [13], in which $\bar{H}_f$ increases from 250 kOe for $x = 0$ to 278.5 kOe for $x = 0.7$ and then decreases to 262 kOe for $x = 0.9$.

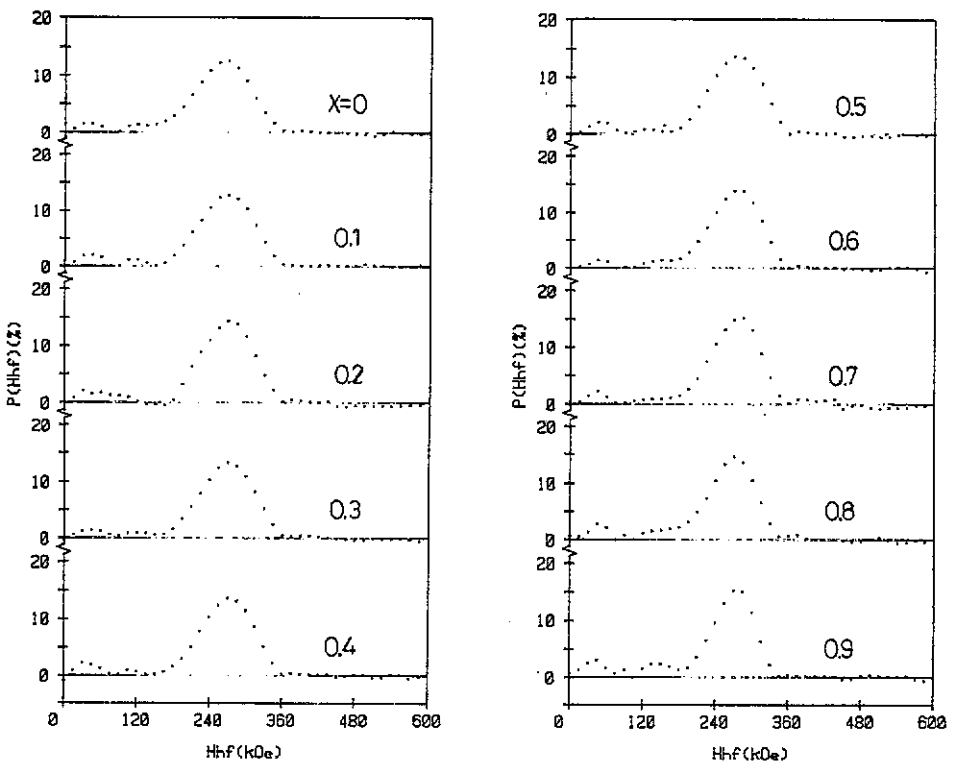

Figure 5. Magnetic hyperfine field distribution $P(H)$ of $(Fe_{1-x}Co_x)_{77.5}Nd_4B_{18.5}$ amorphous alloys at 77 K.

3.2. Curie temperature

Figure 6 shows the temperature dependence of the saturation magnetization σ_s of amorphous $(Fe_{1-x}Co_x)_{77.5}Nd_4B_{18.5}$ alloys. For $x \geqslant 0.4$, the Curie temperature T_C of the samples is higher than the crystallization temperature. The Curie temperature T_C of amorphous samples is obtained by linear extrapolation of the squared

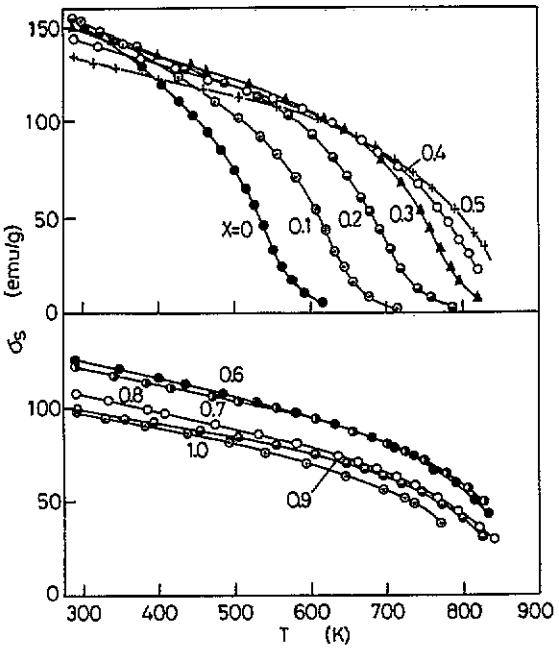

Figure 6. Temperature dependence of the saturation magnetization σ_s of amorphous $(Fe_{1-x}Co_x)_{77.5}Nd_4B_{18.5}$ alloys.

magnetization σ_s^2 versus temperature curves to $\sigma_s^2 = 0$. For $x \leqslant 0.3$, the values of T_C obtained by this method are in agreement with those determined from the temperature dependence of the AC susceptibility.

Figure 2(*b*) shows the Curie temperature T_C for $(Fe_{1-x}Co_x)_{77.5}Nd_4B_{18.5}$ amorphous alloys as a function of Co concentration. The Curie temperature is found to increase at first and then to decrease with increasing Co concentration. T_C has a wide maximum value of 895 K at about $x = 0.7$. The result shown in figure 2(*b*) is very similar to those for other amorphous Fe–Co-based alloys [10]. The variation in T_C with transition-metal content for a fixed metalloid composition may be systematized using the phenomenological model described by Kouvel [14]. Following Kouvel, the Curie temperature T_C of amorphous $(Fe_{1-x}Co_x)_{77.5}Nd_4B_{18.5}$ can be deduced to be

$$T_C = \tfrac{1}{2}[T_{Fe-Fe}(1-x)+T_{Co-Co}x]+\{\tfrac{1}{4}[T_{Fe-Fe}(1-x)-T_{Co-Co}x]^2+T_{Fe-Co}^2(1-x)x\}^{1/2} \quad (4)$$

where T_{Fe-Fe}, T_{Co-Co} and T_{Fe-Co} are the interaction temperatures for Fe–Fe, Co–Co and Fe–Co atom pairs and represent the magnitude of the exchange interactions between the atoms. By assuming that $T_{Fe-Co} = T_{Co-Fe}$, the Curie temperature was calculated and shown in figure 2(*b*) as a full curve. This best fit to the experimental data was obtained with $T_{Fe-Fe} = 584$ K, $T_{Co-Co} = 825$ K and $T_{Fe-Co} = 1010$ K. The exchange interaction for the Fe–Co atom pair is much stronger than those for the Fe–Fe and Co–Co atom pairs in amorphous $(Fe_{1-x}Co_x)_{77.5}Nd_4B_{18.5}$ alloys and hence T_C exhibits a maximum. This feature is exceptionally similar to the behaviour of other amorphous Fe–Co-based alloys, such as $(Fe_{1-x}Co_x)_{78}Si_{10}B_{12}$ and $(Fe_{1-x}Co_x)_{80}P_{13}C_7$, in which T_{Fe-Co} is larger than T_{Fe-Fe} and T_{Co-Co} [10].

3.3. Crystallization behaviours

DSC curves for amorphous $(Fe_{1-x}Co_x)_{77.5}Nd_4B_{18.5}$ alloys show two exotherms for

$x \leqslant 0.7$ and only a sharp exotherm for $x \geqslant 0.8$. The first exotherm originates from the crystallization of amorphous alloys, and the second exotherm corresponds to the transformation of a certain metastable phase. The first exothermic peak temperature T_{m1} and the second exothermic peak temperature T_{m2} obtained from DSC measurement at a heating rate of 20 K min^{-1} are shown in figure 7 as functions of the Co concentration x. The crystallization temperature of the samples is found to be approximately constant when the Co concentration is varied from $x = 0$ to $x = 0.7$ and then to increase slightly with increasing Co concentration. This result implies that the thermal stability of amorphous $(Fe_{1-x}Co_x)_{77.5}Nd_4B_{18.5}$ alloys is only a little influenced by the Co concentration.

X-ray diffraction patterns of the crystallized $(Fe_{1-x}Co_x)_{77.5}Nd_4B_{18.5}$ alloys annealed at 670 °C for 2 min are shown in figure 8. For $x = 0$, x-ray diffraction patterns of samples exhibit Fe_3B lines and some lines from an unidentified phase or phases. Magnetization as a function of temperature shows three magnetic transitions at about 573 K, 780 K and 1043 K, corresponding to the Curie temperatures of $Nd_2Fe_{14}B$, Fe_3B and α-Fe, respectively [4]. For $x < 0.3$, these three magnetic transition temperatures were found to increase with increasing Co concentration, but their x-ray diffraction patterns remain unchanged. This proved that the Co atoms enter the $Nd_2Fe_{14}B$, Fe_3B and α-Fe lattices, forming the $Nd_2(Fe, Co)_{14}B$, $(Fe, Co)_3B$ and α-(Fe, Co) phases [9]. When the Co concentration x is greater than 0.3, the samples crystallized from amorphous show an unidentified phase or phases coexisting with α-(Fe, Co), but the $Nd_2(Fe, Co)_{14}B$ and $(Fe, Co)_3B$ phases vanish. Figure 9 shows x-ray diffraction patterns of some crystallized $(Fe_{1-x}Co_x)_{77.5}Nd_4B_{18.5}$ alloys after annealing at 845 °C for 60 min. The crystalline phases observed by x-ray diffraction measurements are summarized in table 1. It is apparent that the sample with $x = 0$ consists of Fe_3B, Fe_2B, $Nd_{1.1}Fe_4B_4$ (T_2) and α-Fe; the diffraction lines of the $Nd_2Fe_{14}B$ phase are indistinguishable. In the samples containing Co, the amounts of $(Fe, Co)_3B$ and T_2 phases decrease rapidly and disappear at $x > 0.1$; the amounts of α-(Fe, Co) increase monotonically with increasing x. The lines of Fe_2B in the x-ray diffraction patterns do not appear to shift with increasing x; the amount of Fe_2B increases with increasing x until $x = 0.1$, then decreases markedly and finally disappears at $x > 0.4$. When the Co concentration x is greater than 0.2, an unidentified phase (or phases) appears. For the samples with a high Co concentration $x \geqslant 0.9$, the x-ray diffraction patterns show only the FCC Co phase and unidentified phases.

3.4. Hard magnetic properties

The amorphous $(Fe_{1-x}Co_x)_{77.5}Nd_4B_{18.5}$ alloys are magnetically soft with a room-temperature coercive field of about 10 Oe for all x. Pronounced effects of heat treatment on magnetic hardness are found. For $x \leqslant 0.3$, when the samples are annealed, the room-temperature coervice field H_c and magnetic energy product $(BH)_{max}$ as functions of annealing temperature T_a both exhibit a maximum value. The optimal annealing temperature is just near the second exothermic peak temperatures in the DSC curves. Figure 10 shows the room-temperature H_c and $(BH)_{max}$ obtained under optimal annealing conditions as functions of Co concentration x. H_c and $(BH)_{max}$ are found to decrease montonically with increasing Co concentration x but exhibit higher values at low Co concentrations. A coercive field of 3 kOe and an energy product of 13.5 MGOe are obtained for the sample with $x = 0.06$ after annealing at 650 °C for 2 min [9]. For $x \geqslant 0.4$, the room-temperature H_c and $(BH)_{max}$ show low values over the wide annealing temperature range $T_a \leqslant 800$ °C. The measurements on

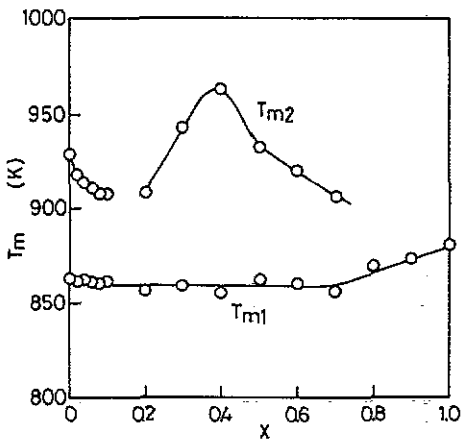

Figure 7. First exothermic peak temperature T_{m1} and second exothermic peak temperature T_{m2} obtained from DSC measurement at a heating rate of 20 K min^{-1} for $(Fe_{1-x}Co_x)_{77.5}Nd_4B_{18.5}$ amorphous alloys as functions of the Co concentration x.

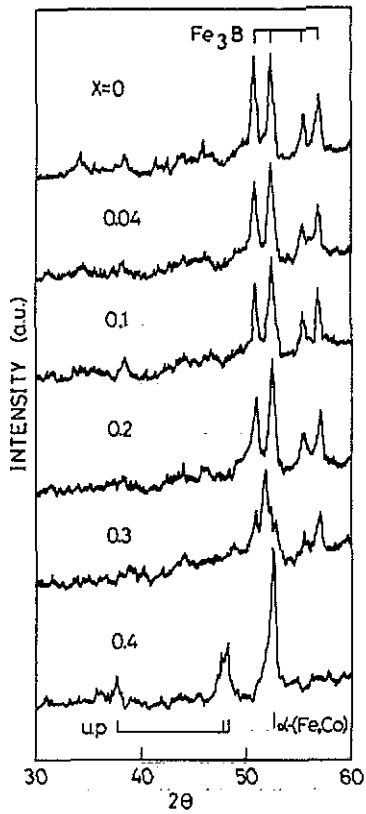

Figure 8. X-ray diffraction patterns of crystallized $(Fe_{1-x}Co_x)_{77.5}Nd_4B_{18.5}$ alloys with $x \leqslant 0.4$ after annealing at 670 °C for 2 min (a.u., arbitrary units).

the temperature dependence of the saturation magnetization show that the optimally annealed samples with a low Co concentration are composed of Fe_3B and $Nd_2Fe_{14}B$ in addition to a small amount of α-Fe. For the zero-Co-content alloy, H_c is found to decrease linearly with increasing temperature to zero at the Curie temperature of $Nd_2Fe_{14}B$. When Co is added to $Fe_{77.5}Nd_4B_{18.5}$, the Curie temperature of the hard magnetic 2:14:1 phase increases with increasing x from 573 K for $x = 0$ to 690 K for $x = 0.2$. The hard magnetic properties of the crystallized samples are related to the presence of the hard magnetic 2:14:1 phase [9]. When the Co concentration is greater than 31 at.% ($x \geqslant 0.4$), the low coercive field and low energy product may be due to the disappearance of the 2:14:1 phase.

4. Conclusion

(i) The magnetic moment $\bar{\mu}_{Fe}$ per Fe atom first increases and then decreases with increasing Co concentration, when the magnetic moment $\bar{\mu}_{Co}$ per Co atom is

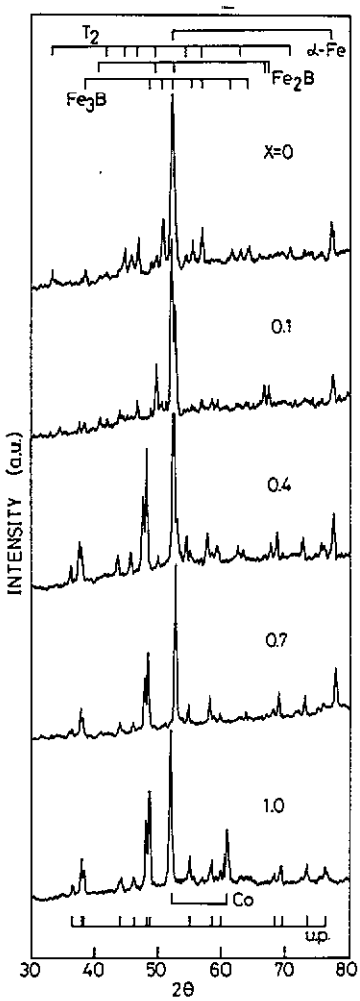

Figure 9. X-ray diffraction patterns of crystallized $(Fe_{1-x}Co_x)_{77.5}Nd_4B_{18.5}$ alloys annealed at 845 °C for 60 min (a.u., arbitrary units).

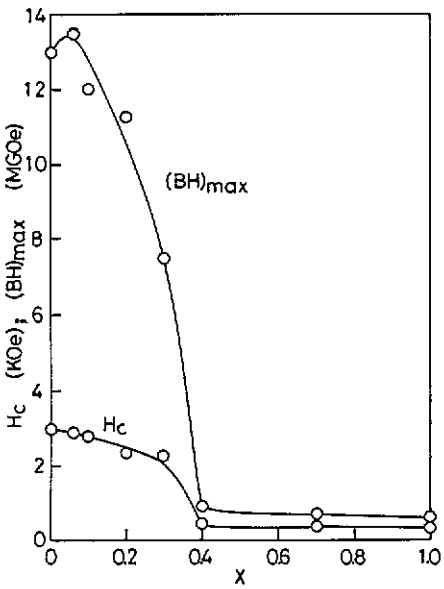

Figure 10. Room-temperature coercive field H_c and maximum energy product $(BH)_{max}$ obtained under optimal annealing conditions for amorphous $(Fe_{1-x}Co_x)_{77.5}Nd_4B_{18.5}$ alloys as functions of Co concentration x.

assumed to be constant. This variation in $\bar{\mu}_{Fe}$ is in good agreement with the Co concentration dependence of the average hyperfine field.

(ii) The Curie temperature increases with increasing Co concentration x, goes through a maximum value of 895 K at $x = 0.7$ and then decreases. The exchange interaction for the Fe–Co atom pair is much stronger than those for the Fe–Fe and Co–Co atom pairs, resulting in a maximum value of the Curie temperature.

(iii) The crystallization temperature measurements show that the thermal stability of this amorphous alloy system is only a little influenced by the Co concentration.

(iv) A high room-temperature coercive field H_c and high maximum energy product $(BH)_{max}$ are exhibited at low Co concentrations. The hard magnetic properties are related to the presence of the hard magnetic 2:14:1 phase.

Table 1. Crystalline phases observed by x-ray diffraction in the amorphous $(Fe_{1-x}Co_x)_{77.5}Nd_4B_{18.5}$ alloys after annealing at 845 °C for 60 min: $T_2 \equiv Nd_{1.1}Fe_4B_4$; UP, unidentified phase or phases.

x	Crystalline phases				
0	Fe_3B	Fe_2B	T_2	α-Fe	
0.06	$(Fe, Co)_3B$	Fe_2B	T_2	α-(Fe, Co)	
0.1		Fe_2B	T_2	α-(Fe, Co)	
0.2		Fe_2B		α-(Fe, Co)	UP
0.3		Fe_2B		α-(Fe, Co)	UP
0.4		Fe_2B		α-(Fe, Co)	UP
0.5				α-(Fe, Co)	UP
0.6				α-(Fe, Co)	UP
0.7				α-(Fe, Co)	UP
0.8				α-(Fe, Co)	UP
0.9				FCC Co	UP
1.0				FCC Co	UP

Acknowledgments

This work is supported by the State Key Laboratory for Rapidly Solidified Non-equilibrium Alloys, Institute of Metal Research, Chinese Academy of Sciences, Shenyang 110015, People's Republic of China. The authors wish to express their gratitude to Zhang Jun-xian, Ning Tai-shan, Wo Feng, Fan Shi-yong, Liang Bing, Yu Xiao-yun and Meng Li-qin for their assistance in preparing the samples used in this study and the magnetic parameter measurements.

References

[1] Coehoorn R, De Mooij D B, Duchateau J P W B and Buschow K H J 1988 *J. Physique Coll.* **49** C8 669
[2] Coehoorn R and De Waard C 1990 *J. Magn. Magn. Mater.* **83** 228
[3] Shen B G, Yang L Y, Zhang J X, Gu B X, Ning T S, Wo F, Zhao J G, Guo H Q and Zhan W S 1990 *Solid State Commun.* **74** 893
[4] Shen B G, Zhang J X, Yang L Y, Wo F, Ning T S, Ji S Q, Zhao J G, Guo H Q and Zhan W S 1990 *J. Magn. Magn. Mater.* **89** 195
[5] Zhang J X, Shen B G, Yang L Y and Zhan W S 1990 *Phys. Status Solidi* a **122** 651
[6] Yang L Y, Shen B G, Zhang J X, Wo F, Ning T S, Zhao J G, Guo H Q and Zhan W S 1990 *J. Less-Common Met.* **166** 189
[7] Coey J M D, Chappert J, Rebouillat J P and Wang T S 1976 *Phys. Rev. Lett.* **36** 1061
[8] Shen B G, Zhang J X, Yang L Y, Guo H Q and Zhao J G 1991 *Mater. Sci. Eng.* A **133** 162
[9] Shen B G, Yang L Y, Zhang J X, Wo F, Ning T S, Zhao J G, Guo H Q and Zhan W S 1991 *J. Magn. Magn. Mater.* **96** 335
[10] Luborsky F E 1980 *Ferromagnetic Materials* vol 1, ed E P Wohlfarth (Amsterdam: North-Holland) p 482
[11] Dai D S, Fang R Y, Tong L T, Liu Z X, Zhou Z J and Lin Z H 1985 *J. Appl. Phys.* **57** 3589
[12] Collins M F and Forsyth J B 1963 *Phil. Mag.* **8** 401
[13] Guo H Q, Shen B G, Yu B L, Zhan W S and Pan X S 1984 *Acta Metal. Sin.* **20** B205
[14] Kouvel J S 1969 *Magnetism and Metallurgy* vol 2, ed A E Berkowitz and E Kneller (New York: Academic) pp 523–75